Simulation of the Optical Absorption Spectra of Gold Nanorods as a Function of Their Aspect Ratio and the Effect of the Medium Dielectric Constant

S. Link, M. B. Mohamed, and M. A. El-Sayed*

Laser Dynamics Laboratory, School of Chemistry and Biochemistry, Georgia Institute of Technology, Atlanta, Georgia 30332-0400

Received: January 13, 1999; In Final Form: March 2, 1999

Gold nanorods with different aspect ratios are prepared in micelles by the electrochemical method and their absorption spectra are modeled by theory. Experimentally, a linear relationship is found between the absorption maximum of the longitudinal plasmon resonance and the mean aspect ratio as determined from TEM. It is shown here that such a linear dependence is also predicted theoretically. However, calculations also show that the absorption maximum of the longitudinal plasmon resonance depends on the medium dielectric constant in a linear fashion for a fixed aspect ratio. Attempts to fit the calculations to the experimental values indicate that the medium dielectric constant has to vary with the aspect ratio in a nonlinear way. Chemically, this suggests that the structure of the micelle capping the gold nanorods is size dependent. Furthermore, comparison with the results obtained for rods of different aspect ratios made by systematic thermal decomposition of the long rods further suggests that the medium dielectric constant is also temperature dependent. This is attributed to thermal annealing of the structure of the micelles around the nanorods.

Introduction

In recent years the interest in the preparation and characterization of nanostructured materials has grown constantly because of their distinctive properties and potential use in technological applications.[1,2] Since the electronic, magnetic, and catalytic properties of these particles depend mainly on their size and shape, one of the desired goals is to control the morphology of metal and semiconductor nanoparticles.[1−3] Shape control has successfully been demonstrated for platinum nanoparticles[4] as well as for metallic carbide nanotubes.[5−8] Furthermore, gold nanorods have recently been prepared by electrodeposition of gold into nanoporous alumina[9−11] and by an electrochemical method with the aid of shape-inducing micelles.[12]

In addition to the recent interest in the shape control of nanoparticles, the optical properties of noble metal particles with their intense colors have fascinated scientists since the turn of this century.[13,14] For example, spherical gold nanoparticles show a strong absorption band in the visible region of the electromagnetic field at about 520 nm. This absorption, called the plasmon absorption,[15,16] is absent for very small particles (2 nm and smaller) as well as for bulk gold. It originates from the oscillation of the free electrons (6s-electrons of the conduction band in the case of gold). Mie[13] first described this phenomenon theoretically by solving Maxwell's equations for a radiation field interacting with a spherical metal particle under the appropriate boundary conditions. The only material-related functions and constants in Mie's theory are the complex dielectric function of the metal and the dielectric constant of the surrounding medium. The plasmon absorption band also depends on the size of the particles and many attempts have been made to experimentally correlate the absorption maximum and the plasmon bandwidth to the actual particle size with overall moderate success.[17−20] An inhomogeneous size distribution and different surrounding media in various studies complicate the correlation between theory and experiment.[17,18,21] The surrounding medium, often referred to as the capping material, is however of great importance as it prevents aggregation followed by precipitation of gold and other metal particles in solution.

Gans[14] extended Mie's theory to prolate and oblate spheroidal particles averaged over all orientations. For gold nanorods the plasmon resonance then splits into two modes: one longitudinal mode along the long axis of the rod and a transverse mode perpendicular to the first. Maxwell−Garnett theory,[16,17,22] an effective medium theory, is also often used to describe the optical properties of metallic nanoparticles. Maxwell−Garnett theory computes the effective (complex) dielectric function of the composite material consisting of the metallic nanoparticles and the surrounding medium (host material). From this dielectric function the refractive index and the absorption can be calculated. The shape of the particles can be included in this theory by a screening parameter. Martin and co-workers[9,23−26] have used and modified the Maxwell−Garnett theory to model the absorption spectra of gold nanoparticles with shapes that vary from oblate or pancakelike to prolate or needlelike. The gold nanorods are embedded in a porous aluminum oxide membrane, in which they are well separated and aligned parallel to each other. The optical absorption spectrum shows only one plasmon band, which blue-shifts with increasing aspect ratio in agreement with the theoretical simulations.

We have used Gans' theory together with the known dielectric function for gold[27] and modeled the optical absorption spectra of several colloidal gold nanorod samples with varying aspect ratios. We were able to derive a simple relationship between the absorption maximum of the longitudinal plasmon resonance and the aspect ratio and the medium dielectric constant. A linear dependence of the absorption maximum on the aspect ratio as well as on the medium dielectric constant was found for a constant value of the other parameter. Comparison with experimental results, where the mean aspect ratio was determined by transmission electron microscopy (TEM), indicates

* Author to whom correspondence should be addressed.

10.1021/jp990183f CCC: $18.00
Published on Web 04/02/1999

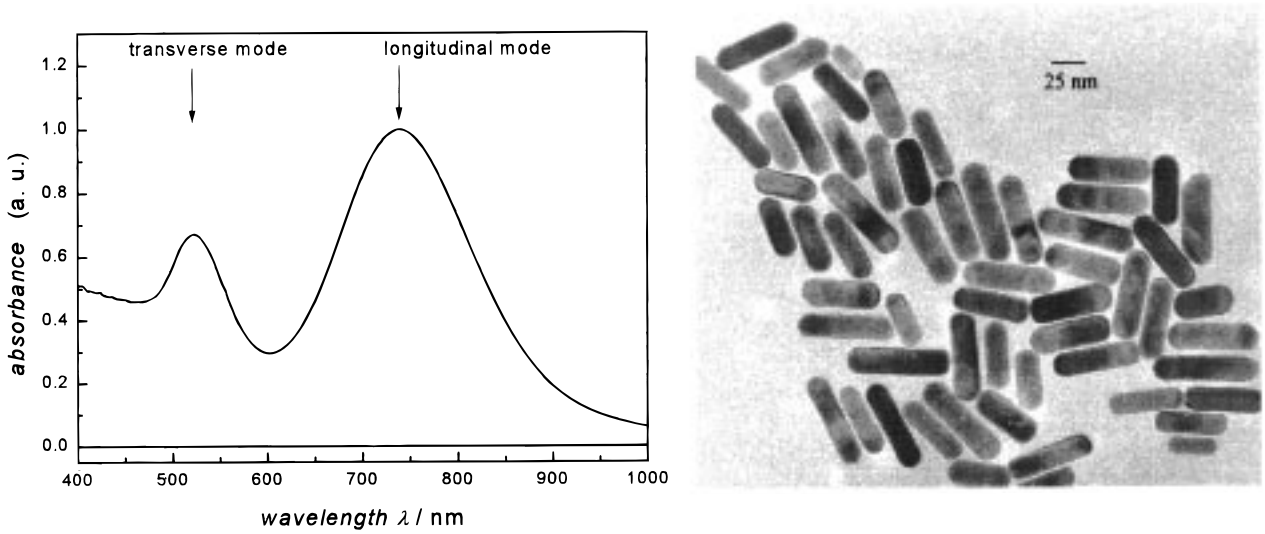

Figure 1. Left: Experimental UV−vis absorption spectrum of a gold nanorod sample with an average aspect ratio of 3.3. The band at 525 nm is referred to as the transverse plasmon resonance, while the one centered at 740 nm is called the longitudinal plasmon absorption. Right: TEM image of the same solution.

that the organization of the capping material surrounding the gold nanorods differs for rods with different aspect ratios. Furthermore, the fact that the absorption maximum of a certain rod having a specific aspect ratio is found to depend on its method of preparation (either by adjusting the conditions of the method or starting with a distribution of larger rods and thermally changing it to the distribution required[28]) suggests that the organization of the micelles around the nanorods is kinetically and not thermodynamically controlled.

Experimental Section

The gold nanorods were prepared in micelles using an electrochemical method described previously.[12] The electrochemical cell consisted of a gold (anode) and a platinum plate (cathode). An additional silver plate is placed behind the Pt electrode. The electrolyte solution consisted of a hydrophilic cationic surfactant, hexadecyltrimethylammonium bromide, and a hydrophobic cationic cosurfactant, tetradecylammonium bromide or tetraoctylammonium bromide. The ratio between these surfactants controls the average aspect ratio of the gold nanorods. The electrolysis was carried out for 45 min with an applied current of 5 mA at a temperature of 42 °C and under constant ultrasonication. The nanorods were separated from spherical nanoparticles by centrifugation.

The UV−vis absorption spectra were recorded on a Beckman DU 650 spectrophotometer. The size and shape distributions of the nanorods were determined from the TEM images of the evaporated solutions on carbon-coated copper grids. A Hitachi HF-2000 field emission TEM operating at 200 kV was used. Normally, 300 particles were counted in determining the distributions for each sample.

Results

Figure 1 shows the absorption spectrum and a TEM image of one of the prepared samples. The average aspect ratio of these nanorods is 3.3 and they have two absorption maxima at 525 and 740 nm corresponding to the transverse and longitudinal mode, respectively. This sample was also used for the thermal reshaping studies presented elsewhere.[28] Seven more gold nanorod samples were prepared by the method described in the Experimental Section. Their average aspect ratio was controlled by the ratio of surfactant molecules to cosurfactant molecules. The average aspect ratios and the absorption maxima of their longitudinal plasmon resonance are listed in Table 1.

Using an extension of the Mie theory it is attempted here to explore theoretically the relationship between the aspect ratio of the gold nanorods and the position of this absorption maximum. According to Gans,[14,29] the extinction coefficient γ of randomly oriented particles in the dipole approximation is

$$\gamma = \frac{2\pi NV\epsilon_m^{3/2}}{3\lambda}\sum_j \frac{(1/P_j^2)\epsilon_2}{\left(\epsilon_1 + \frac{1-P_j}{P_j}\epsilon_m\right)^2 + \epsilon_2^2} \tag{1}$$

where N is the number of particles per unit volume, V the volume of each particle, ϵ_m the dielectric constant of the surrounding medium, λ the wavelength of the interacting light, and ϵ_1 and ϵ_2 are the real and complex part of the material dielectric function. The latter one is frequency dependent, while ϵ_m is assumed to be a constant. P_j are the depolarization factors for the three axes A, B, C of the rod with $A > B = C$. They are defined as

$$P_A = \frac{1-e^2}{e^2}\left[\frac{1}{2e}\ln\left(\frac{1+e}{1-e}\right) - 1\right] \tag{2}$$

$$P_B = P_C = \frac{1-P_A}{2} \tag{3}$$

where

$$e = \sqrt{1 - \left(\frac{B}{A}\right)^2} \tag{4}$$

The ratio A/B is the aspect ratio R.

With the known values for the complex dielectric constant of gold,[27] eq 1 is plotted in Figure 2 for different aspect ratios while the medium dielectric constant was fixed to a value of 4. It can be seen that two maxima are present in the simulated absorption spectra corresponding to the transverse and longitudinal resonances. The absorption maximum of the transverse mode shifts to shorter wavelength with increasing aspect ratio. This trend for the transverse mode of the surface plasmon

TABLE 1: Absorption Maximum of the Longitudinal Plasmon Resonance λ_{max} and Average Aspect Ratio R of the Electrochemically Prepared Gold Nanorod Samples and the Respective Values Obtained by Thermal Reshaping

preparation			thermal reshaping		
λ_{max}	R	ϵ_m[a]	λ_{max}	R	ϵ_m[a]
780 nm	3.7	4.0	740 nm	3.3	4.2
749 nm	3.5	3.9	722 nm	2.9	5.0
740 nm	3.3	4.2	700 nm	2.6	5.6
709 nm	3.0	4.3	682 nm	2.3	6.9
673 nm	2.7	4.6			
660 nm	2.65	4.4			
656 nm	2.5	4.8			
610 nm	2.1	6.0			

[a] The medium dielectric constant ϵ_m was calculated as outlined in the text.

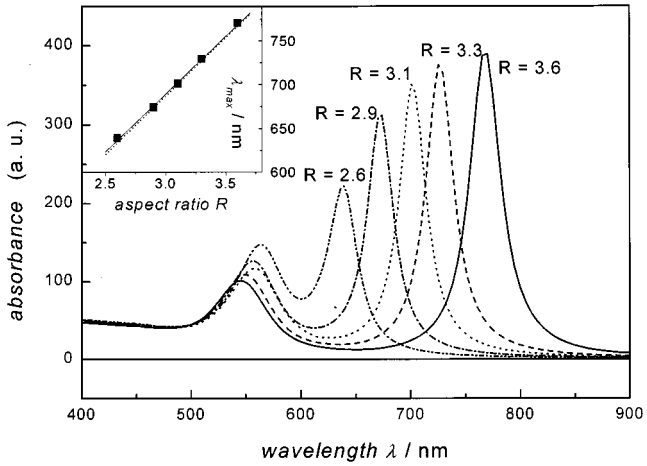

Figure 2. Calculated absorption spectra of elongated ellipsoids with varying aspect ratios R using eq 1. The medium dielectric constant was fixed at a value of 4. The inset shows a plot of the maximum of the longitudinal plasmon band determined from the calculated spectra as a function of the aspect ratio. The solid line is a linear fit to the data points. The dotted line is a plot of eq 8 with a medium dielectric constant of 4.

oscillation of randomly orientated nanorods predicted by Gans' theory is in agreement with the results of Martin and co-workers,[9,23−26] who also find a blue-shift of the plasmon maximum using Maxwell−Garnett theory. On the other hand, the absorption maximum of the longitudinal mode red-shifts with increasing gold nanorod aspect ratio. However, the effect on the longitudinal mode is much more pronounced showing a variation of over 100 nm. Furthermore, the relative intensity ratio of the longitudinal to the transverse mode increases with increasing aspect ratio.

In Figure 3 eq 1 is plotted for different values of the medium dielectric constant with a fixed aspect ratio of 3.3. In this case both maxima shift to longer wavelength and the intensity of both resonances increases with an increasing medium dielectric constant. Again, the longitudinal mode is more sensitive. Therefore the remaining discussion will be limited to the longitudinal mode only. This is also justified by the fact that the absorption band in the experimental spectrum is a superposition of the transverse mode of the nanorods and the plasmon absorption of the spherical gold particles that are present in solution as impurities in the rod synthesis.

In the insets of Figures 2 and 3, the absorption maximum of the longitudinal resonance is plotted against the aspect ratio and the medium dielectric constant, respectively. The solid lines represent linear fits to the points, which were determined from the calculated absorption spectra. This clearly demonstrates that

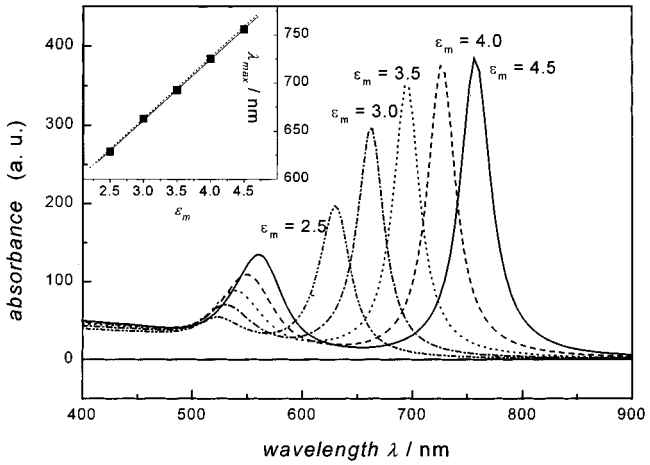

Figure 3. Calculated absorption spectra of elongated ellipsoids with varying medium dielectric constant ϵ_m using eq 1. The aspect ratio was fixed at a value of 3.3. The inset shows a plot of the maximum of the longitudinal plasmon band determined from the calculated spectra as a function of the medium dielectric constant. The solid line is a linear fit to the data points. The dotted line is a plot of eq 8 with a aspect ratio of 3.3.

the relationship between the absorption maximum of the longitudinal mode and the aspect ratio and the medium dielectric constant can be regarded as linear for the range examined in Figures 2 and 3. (The fit in Figure 2 has a regression coefficient of $r = 0.99928$, and in Figure 3 $r = 0.99989$). This is an important conclusion because it cannot be seen directly by considering eqs 1−4. It especially shows that the effect of the medium dielectric constant should not be underestimated.

If these linear dependencies hold, then it would further be interesting to derive an equation which allows us to predict the absorption maximum of the longitudinal mode for a certain aspect ratio and dielectric constant instead of calculating the whole absorption spectrum. This can be done by considering that the resonance condition for the longitudinal mode is roughly fulfilled if[29]

$$\epsilon_1 = -\frac{(1 - P_A)\epsilon_m}{P_A} \tag{5}$$

The real part of the gold dielectric function ϵ_1 is wavelength dependent. However, a plot of ϵ_1 vs the wavelength of the interacting light in the interesting range between 500 and 800 nm is found to be nearly linear, and a fit gives the following values for the intercept and slope with a regression coefficient of 0.99956:

$$\epsilon_1(\lambda) = 34.66 - 0.07\lambda \tag{6}$$

Similarly, plotting $(1 - P_A)/P_A$ as a function of the aspect ratio R between 2 and 4 and linearizing yields

$$\frac{1 - P_A}{P_A} = -3.40 + 2.45R \tag{7}$$

with a regression coefficient of 0.99846. Combining eqs 5−7 then gives

$$\lambda_{max} = 33.34\,\epsilon_m R - 46.31\,\epsilon_m + 472.31$$
$$= (33.34R - 46.31)\epsilon_m + 472.31 \tag{8}$$

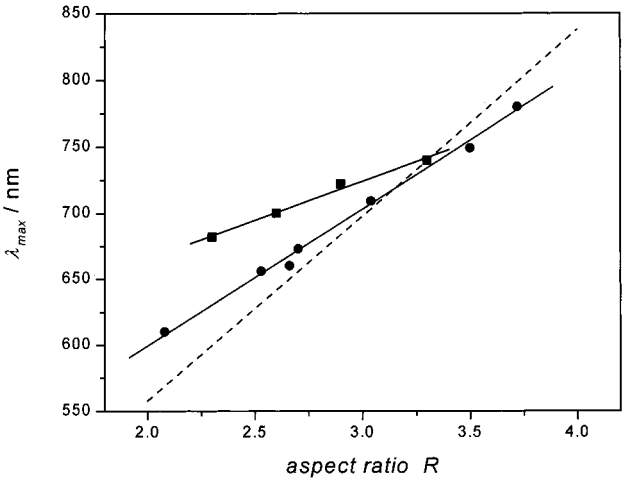

Figure 4. Plot of the absorption maximum of the longitudinal plasmon resonance against the aspect ratio as determined by TEM. The circles correspond to different preparations while the squares are the results obtained by thermal reshaping. The solid lines are linear fits to the experimental data points. The dashed line corresponds to eq 8 with a medium dielectric constant of 4.2. This value was chosen as to match the sample shown in Figure 1, which was also used for the thermal reshaping studies ($R = 3.3$, $\lambda_{max} = 740$ nm).

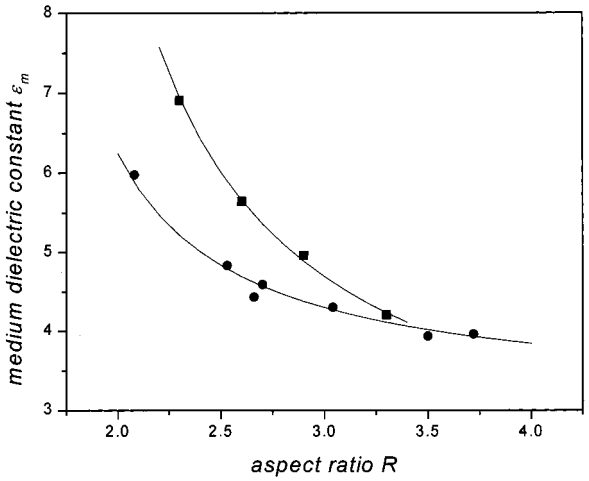

Figure 5. Dependence of the medium dielectric constant on the aspect ratio obtained if the medium dielectric constant is used as a variable parameter to match the experimental absorption maximum of the longitudinal plasmon resonance. The circles correspond to different preparations while the squares are the results obtained by thermal reshaping. The solid lines are obtained with the help of the linear regressions in Figure 4 as explained in the text (eqs 9 and 10).

Equation 8 is plotted in the insets of Figures 2 and 3 as the dotted line for a fixed dielectric constant of 4 and a fixed aspect ratio of 3.3, respectively. Very good agreement is found with the data points calculated by the full expression of eq 1 even after the two simplifications in eqs 6 and 7 were made. This therefore suggests that the assumptions made in the derivation of eq 8 are acceptable.

Discussion

The theoretical calculations were carried out in order to compare them with experimental data. Especially the relationship between the average nanorod aspect ratio determined by TEM and the absorption maximum of the longitudinal plasmon resonance was of great interest to us. The values of the average aspect ratios and the absorption maxima for the eight different samples prepared electrochemically are given in Table 1 and are also plotted in Figure 4. Indeed, the experimental data points can be described by a linear relationship ($\lambda_{max} = 392.11 + 103.70R$ with $r = 0.99676$) in general agreement with other experimental results.[11,12] Also included in Figure 4 are the experimental data points obtained after thermal reshaping of the sample shown in Figure 1 ($R = 3.3$, $\lambda_{max} = 740$ nm). They follow a linear trend as well ($\lambda_{max} = 547.29 + 58.9R$ with $r = 0.99519$).

Surprisingly neither of the two experimental lines can be matched by eq 8 for a single value of the medium dielectric constant. Varying ϵ_m can reproduce the right slope for either line, but the intercept also depends on ϵ_m. The broken line in Figure 4 is a plot of eq 8 with a medium dielectric constant of 4.2. This value of ϵ_m was chosen in order to match the experimental absorption maximum of the sample with an average aspect ratio of 3.3 which was also used in the thermal reshaping studies and represents a common point for the two experimental lines (same sample as shown in Figure 1).

If the medium dielectric constant is however treated as an adjustable parameter the experimental absorption maxima can be well reproduced for each sample by eq 8. This would then mean that the medium dielectric constant becomes size dependent and varies in a nonlinear fashion with the aspect ratio as shown in Figure 5. ϵ_m increases with decreasing aspect ratio of the nanorods. The points in Figure 5 were calculated by solving eq 8 with the experimentally determined absorption maxima and aspect ratios for the different samples as listed in Table 1. These values of the medium dielectric constant are also included in Table 1. The solid lines are obtained setting eq 8 equal to the linear regressions in Figure 4 and solving for ϵ_m as a function of the aspect ratio R. This yields the following equations:

$$\epsilon_m = \frac{103.70R - 80.20}{33.34R - 46.31} \tag{9}$$

$$\epsilon_m = \frac{58.99R - 75.02}{33.34R - 46.31} \tag{10}$$

A dependence of the medium dielectric constant on the nanorod aspect ratio means in more chemical terms that the structure of the surrounding micelle is different for different nanorod sizes. The micelle consists of two surfactant molecules, hexadecyltrimethylammonium bromide and tetradecylammonium bromide or tetraoctylammonium bromide, and prevents the nanorods from aggregation and precipitation. Their respective ratio controls the length of the gold nanorods suggesting a different environment for each prepared sample due to a different composition of the micelles. The exact arrangement of the molecules within the micelle and their interaction with the gold surface are however not known at the moment. The assumption that the organization of the molecules at the gold surface might differ for rods of different length seems very reasonable and this in turn would lead to a variation in the effective medium dielectric constant. Values between 3 and 7 for ϵ_m are also very reasonable when compared to other organic chemicals with structures similar to the surfactants used in this study.[30]

From Figures 4 and 5 it is also obvious that the thermal reshaping of the nanorods alters the structure of the micelle surrounding the smaller rods, which stay in solution. A reorganization of the micelle structure due to an elevated temperature causes the gold nanoparticles to have a different effective environment characterized by a higher value for its dielectric constant as monitored by the longitudinal surface plasmon oscillation of the nanorods. This suggests that the structure of the capping micelles of a certain rod at room temperature prepared by thermal reshaping is different from the

one of a freshly prepared sample with the same average aspect ratio. Heating the micellar solution could anneal the structure of the micelles capping the gold nanorods. This suggests that the originally synthesized sample has a micellar structure that is kinetically, rather than thermodynamically, controlled. Heating the solution anneals the structure toward the more stable thermodynamic structure with a higher value of the dielectric constant.

Equation 8 is an excellent approximation for the region considered here (aspect ratio ranging from 2 to 4 and a wavelength range of 500 to 800 nm), but applying this simple theory (dipole approximation) to an inhomogeneously broadened sample and proposing a change of the medium dielectric constant as shown in Figure 5 deserves some caution. Therefore Raman experiments (especially surface-enhanced Raman scattering SERS) should be carried out to test the predictions made in this paper.

A last interesting point which should be raised in this discussion is the fact that eq 1 depends on the aspect ratio only. The actual size of the particles is not considered in this dipole approximation which is usually applicable to sizes of less than 1/10 the wavelength of the interacting light. Our particles have a typical length of about 60 nm and a width of 20 nm and are therefore just within the limit of the dipole approximation. The question however arises if multipole terms have to be considered for larger particles with the same aspect ratio and if the absorption spectrum might change for much smaller particles of the same aspect ratio.

Acknowledgment. This work was supported by the Office of Naval Research (through Grant No. N00014-95-1-0306) and the Georgia Tech Molecular Design Institute (through Grant No. N00014-95-1-1116). S.L. thanks the German Fond der Chemischen Industrie and the German BMBF for a Ph.D. fellowship, and M.B.M. thanks Egyptian GM.

References and Notes

(1) Schmid, G. *Clusters & Colloids: From Theory to Application*; VCH: Weinheim, 1994.

(2) Alivisatos, A. P. *J. Phys. Chem.* **1996**, *100*, 13226.

(3) Henglein, A. *J. Phys. Chem.* **1993**, *97*, 8457.

(4) Ahmadi, T. S.; Wang, Z. L.; Green, T. C.; Henglein, A.; El-Sayed, M. A. *Science* **1996**, *272*, 1924.

(5) Dai, H.; Wong, E. W.; Lu, Z. Y.; Fan, S.; Lieber, C. M. *Nature* **1995**, *375*, 76.

(6) Wong, E. W.; Sheehan, P. E.; Lieber, C. M. *Science* **1997**, *227*, 1971.

(7) Yang, P.; Lieber, C. M. *Science* **1996**, *273*, 1836.

(8) Morales, A. M.; Lieber, C. M. *Science* **1998**, *279*, 208.

(9) Foss, C. A.; Hornyak, G. L.; Tierney, M. J.; Martin, C. R. *J. Phys. Chem.* **1992**, *96*, 9001.

(10) Martin, C. R. *Chem. Mater.* **1996**, *8*, 1739.

(11) v. d. Zande, B. M. I.; Bohmer, M. R.; Fokkink, L. G. J.; Schonenberger, C. *J. Phys. Chem. B* **1997**, *101*, 852.

(12) Yu, Y.; Chang, S.; Lee, C.; Wang, C. R. C. *J. Phys. Chem. B* **1997**, *101*, 6661.

(13) Mie, G. *Ann. Physik* **1908**, *25*, 377.

(14) Gans, R. *Ann. Physik* **1915**, *47*, 270.

(15) Kerker, M. *The Scattering of Light and Other Electromagnetic Radiation*; Academic Press: New York, 1969.

(16) Bohren, C. F.; Huffman, D. R. *Absorption and Scattering of Light by Small Particles*; John Wiley: New York, 1983.

(17) Kreibig, U.; Vollmer, M. *Optical Properties of Metal Clusters*; Springer: Berlin, 1995.

(18) Kreibig, U.; Genzel, U. *Surf. Sci.* **1985**, *156*, 678.

(19) Cini, M. *J. Opt. Soc. Am.* **1981**, *71*, 386.

(20) Alvarez, M. M.; Khoury, J. T.; Schaaff, T. G.; Shafigullin, M. N.; Vezmer, I.; Whetten, R. L. *J. Phys. Chem. B* **1997**, *101*, 3706.

(21) Persson, N. *J. Surf. Sci.* **1993**, *281*, 153.

(22) Maxwell−Garnett, J. C. *Philos. Trans. R. Soc. London* **1904**, *203*, 385.

(23) Foss, C. A.; Hornyak, G. L.; Stockert, J. A.; Martin, C. R. *J. Phys. Chem.* **1992**, *96*, 7497.

(24) Foss, C. A.; Hornyak, G. L.; Stockert, J. A.; Martin, C. R. *J. Phys. Chem.* **1994**, *98*, 2963.

(25) Hornyak, G. L.; Patrissi, C. J.; Martin, C. R. *J. Phys. Chem. B* **1997**, *101*, 1548.

(26) Hornyak, G. L.; Martin, C. R. *Thin Solid Films* **1997**, *303*, 84.

(27) Johnson, P. B.; Christy, R. W. *Phys. Rev. B* **1972**, *6*, 4370.

(28) Mohamed, M. B.; Link, S.; El-Sayed, M. A. *J. Phys. Chem. B* **1998**, *102*, 9370.

(29) Papavassiliou, G. C. *Prog. Solid State Chem.* **1980**, *12*, 185.

(30) Lide, D. R. *Handbook of Chemistry and Physics*, 75th ed.; CRC Press: Boca Raton, 1994.